Available online at www.sciencedirect.com

ScienceDirect

IFAC PapersOnLine 54-7 (2021) 803–808

Modeling and simulation of bimetallic strips in industrial circuit breakers ⋆

L. Maurelli *, **M. Mazzoleni** *, **F. Previdi** *

* *Department of Management, Information and Production engineering University of Bergamo, via Marconi 5, 24044 Dalmine (BG), Italy (e-mail: luca.maurelli@unibg.it).*

Abstract: This paper presents a dynamical model for the dynamics of the bimetallic strip in industrial circuit breakers. The strip acts as thermo-mechanical actuator that opens the circuit breaker in case of overloads. The overall model can be decomposed in two submodels: an electro-thermal and a thermo-mechanical one. The first submodel is derived as a gray-box, while the second one as a black-box. Given the overall estimated model, the final aim is to determine appropriate calibration actions on the device prior to its delivery. The developed model is tested on experimental data of real industrial circuit-breakers.

Keywords: Mechatronic systems.

1. INTRODUCTION

A *thermostatic bimetal* consists of two metal sheets with different coefficients of thermal expansion, welded to form a single strip. The sheet with highest thermal expansion is denoted as the *active* component, while the other one is denoted as the *passive* component. A third metallic layer is often added in-between the two elements, with the aim to improve both electrical and thermal conductivity, see (Webster, 1999, Chapter 32). When heated, the so-called active component expands more than the passive one, causing the bimetallic strip to bend, see Khadkikar (1993). Bimetallic strips are used in a variety of engineering applications as thermo-electrical actuators, such as thermometers and thermostats (Sedighi and Dardashti (2012)), MEMS sensors and actuators (Ross et al. (2005), Suocheng et al. (2015)), micro-machined valves and pumps (Zou et al. (1999)) and circuit breakers.

Circuit breakers are security switches that automatically interrupt a current flow to protect an electrical circuit from overloads and faults, see Balestrero et al. (2010). Depending on the operating voltage of the circuit breaker, different technologies can be leveraged. In the case of low-voltage circuit breakers, a thermo-magnetic unit is usually employed. The thermo-magnetic element detects current overloads by means of: (i) a thermal protection unit; (ii) an electromagnetic protection unit. The former component protects against long-lasting overloads, while the latter one guards against short circuits. Both units act independently and mechanically to open the breaker's contacts.

The thermal unit is mainly composed by: (i) a bimetallic element fixed at an extreme; (ii) a tripping lever. When a voltage overload rises the current flow magnitude, the bimetal layers are heated, causing a deflection of the strip tip. The bending of the bimetal pulls the tripping lever that, in turns, opens the circuit breaker's contacts, see Fig. 1-(Left).

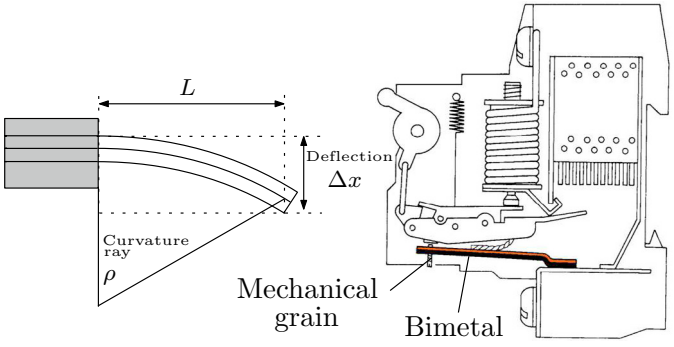

Fig. 1. (Left) Relative deflection Δx for a strip of length L, with curvature ray ρ. (Right) Particular of the mechanical grain component.

The overall bimetal behaviour, specific to circuit breakers, can therefore be divided into two connected compartments:

(1) an Electro-Thermal (ET) dynamics, that relates the effect of the current on the heating of the bimetal;
(2) a Thermo-Mechanical (TM) dynamics, that describes the strip deformation given its temperature.

The modeling of the bimetals dynamics is a topic that has been relatively little addressed in the literature. Since the *electro-thermal dynamics* is peculiar to the circuit breaker application, the research efforts on modeling the bimetal dynamics focused on the *thermo-mechanical dynamics*. Here, the modeling consists in determining two relations: (i) from the strip temperature to its curvature; (ii) from the strip curvature to its vertical displacement (deflection). The first problem was the topic of the seminal work of Timoshenko (1925). The second relation can be formulated by specific assumptions about the geometry of the strip, see e.g. Pionke and Wempner (1991)(Webster, 1999, Chapter 32.1). The before mentioned research works, however,

⋆ The research has been carried in the SMART4CPPS (Smart Solutions for Cyber-Physical Production Systems) project funded by FESR (Fondo Europeo di Sviluppo Regionale).

10.1016/j.ifacol.2021.08.460

presented *static* relations, that may not adequately model experimental data. Dynamic modeling of the thermo-mechanical relations is faced in Čepon et al. (2017) by means of a multi-body approach, and validated by a Finite Element Method (FEM) analysis. However, these models are quite involved: simpler and parameter-lumped representations may be preferred for tailored applications as the one in this work.

The time Δt required for the bimetal to bend and act on the tripping lever is called *trip time*. The trip time can be adjusted by varying the distance between the bimetallic strip and the tripping lever through a *mechanical grain* calibration screw, see Fig. 1-(Right). Due to the geometric variability of the bimetallic strips installed in circuit breakers, manufactures often have to *manually adjust* the calibration screws of their products, in order to provide them with standard opening times. As this goes against the widespread tendency to automate repetitive tasks in production processes, tools that can *automatically regulate the calibration screw*, taking into account the characteristics of each bimetallic strip, are highly envisaged.

To this end, characterizing the overall dynamics of bimetal strips can allow to relate the parameters of a specific bimetal with the most adequate calibration actions to be performed on the mechanical grain. Thus, we propose the following steps towards an automatic calibration of bimetals in circuit breakers:

- estimate a parametric bimetal dynamical model through defined experimental procedures for each circuit breaker;
- given the parameters of the estimated model, perform corrections on the mechanical grain.

The second step can be performed, e.g. by machine learning algorithms, provided that enough data on bimetals and corresponding calibrations are available. This paper focuses on the modeling and estimation step. Specifically:

(1) we develop an *application-oriented* dynamical model of the bimetallic strip in circuit breakers. As far as the authors are aware, this is the first time that an overall modeling (that considers *both* electrical and mechanical dynamics contributions), is performed in this industrial context. The ET dynamics is modeled as a gray-box, while the TM dynamics is modeled with a black-box approach;
(2) we fit and validate the model on experimental data using different circuit breakers. This leads to a set of parameters, specific for each device.

The paper is organized as follows. The experimental setup and data are described in 2. The proposed dynamical model is highlighted in 3. Section 4 presents the model estimation procedure. Section 5 shows the estimation results. Section 6 concludes the paper.

2. TEST BENCH AND EXPERIMENTAL DATA

A total of $N_B = 30$ low-voltage circuit breakers TMAX XT1-3P-R80 were made available by ABB. The following information are measured for each device, see Fig. 2:

- *temperature* T of the bimetal, measured with a thermocouple with sampling time of $t_s = 0.5$ [s];
- *deflection* x of the bimetal, measured with a linear potentiometer with sampling time of $t_s = 0.1$ [s];
- *current indicator* Φ by means of a current probe, that denotes the time instants when the step current input is supplied. The current input is *not measured* but its amplitude is known: in our simulations, we provided a tailored user-generated step input.

By observing transient periods in the current probe data, it is possible to compute:

- *starting time* t_0 of the thermal unit (i.e. when the current supply Φ goes from zero to a nonzero value);
- *trip time* $\Delta t = t_0 - t_{\text{end}}$ of the thermal unit, where t_{end} is selected by looking when the current supply Φ goes from a nonzero to a zero value.

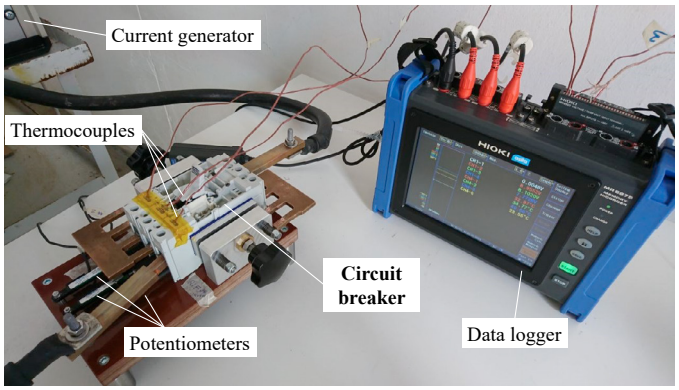

Fig. 2. Experimental setup. It is possible to notice thermocouples and potentiometers attached to each phase of the circuit-breaker.

The nominal rating of the circuit-breaker current is $I_n = 80\,\text{A}$. To simulate an overload on the thermal unit, the current generator was chosen to supply a current peak of $I_p = 200\,\text{A}$ ($k = 2.5$ times the nominal current value).

The test protocol consisted in $N_T = 3$ repetitive tests for each circuit breaker under analysis. Between each consecutive test, the thermal unit was cooled in order to reset the temperature of its bimetal elements to the ambient value. Each circuit-breaker presents $N_P = 3$ phases (every phase corresponds to a single bimetal element), so that the actual bimetallic actuator is composed by N_P bimetal elements. So, a total of $N_C = N_B \cdot N_T \cdot N_P = 270$ curves of temperature and deflection were obtained.

An example of data acquired with this test protocol is depicted in Fig. 3 where the raw dataset for a single circuit-breaker spanning multiple tests is shown. The considered deflection and temperature curves are the data inside the times where the current is active. The temperature curves of the different breaker's phases, along with boxplots of overall trip times and temperatures at the end of the bimetallic trips are depicted in Fig. 4. The deflection curves and the boxplot of the deflection at the end of the bimetal trip are reported in Fig. 5.

Remark 1. (*Pre-processing*) The temperature curves in Fig. 4 were resampled to match the sampling time of the deflection curves $t_s = 0.1\,\text{s}$. Furthermore, the deflection curves in Fig. 4 were obtained by applying an offset to set 0 mm as starting value for all the curves, and converted to increasing values of deflection.

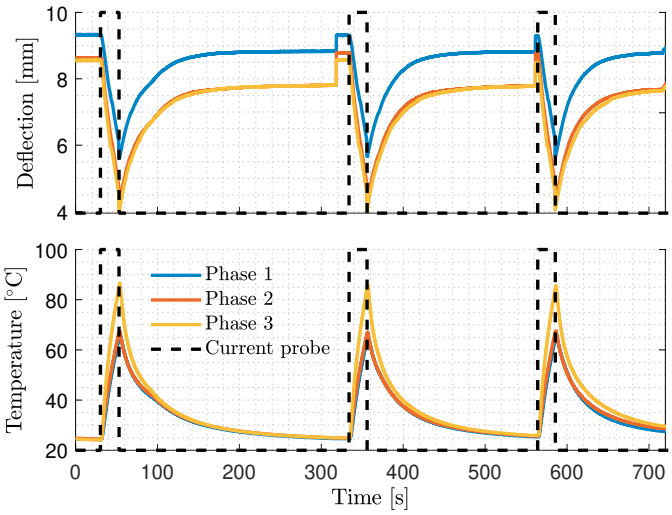

Fig. 3. Example of raw data for a single circuit breaker spanning multiple tests.

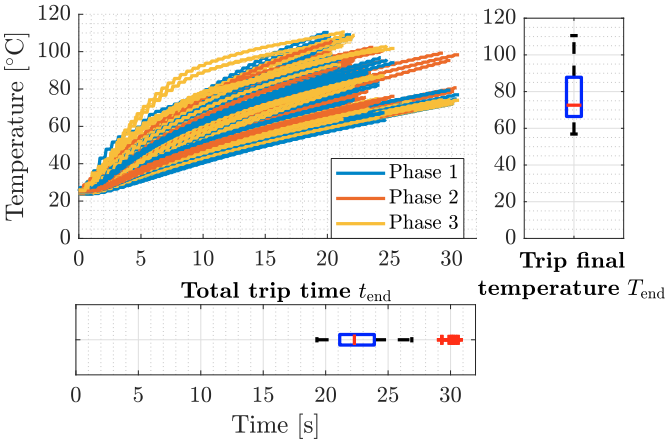

Fig. 4. Experimental temperature curves and boxplots.

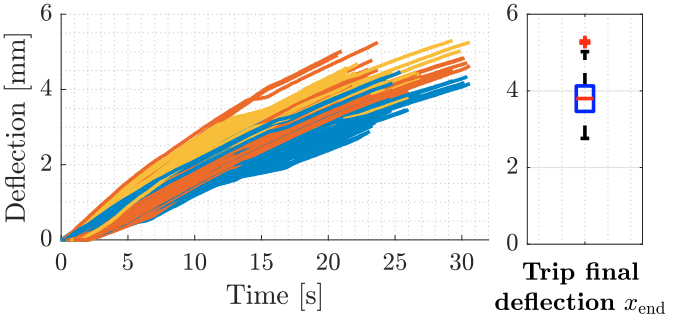

Fig. 5. Experimental deflection curves and boxplots.

A series of statistics were computed on the experimental data in order to summarize their characteristics, such as

$$\Delta x = x_{\text{end}} - x_0 = x_{\text{end}}, \tag{1a}$$
$$\Delta T = T_{\text{end}} - T_0, \tag{1b}$$
$$\Delta t = t_{\text{end}} - t_0 = t_{\text{end}}, \tag{1c}$$

where x_0, T_0, t_0 and $x_{\text{end}}, T_{\text{end}}, t_{\text{end}}$ denote the starting and final values of displacement, temperature and time, respectively.

Remark 2. (*Trip time variability*) The boxplot of the total trip time t_{end} in Fig. 4 shows two groups of experimental data. The first one behaves as standard and contains the median value of 22.5 s. On the other hand, the second one contains abnormal values around 30 s that are clearly separated from the first group. This relates to the project aim to reduce the variability of the trip time to a desired opening target range, by means of the calibration screw.

3. BIMETALLIC STRIP DYNAMICAL MODEL

3.1 Electro-thermal model

The electro-thermal (ET) model that describes the relationship between the current flowing through the bimetal and its temperature rise is derived by modeling the bimetal as a resistor with rectangular cross section. The derivation is based on a energy balance on the bimetallic component. For this reason, the integral form of the thermo-dynamical laws were considered:

$$Q = Q^+ - Q^- \tag{2}$$

where the heat accumulated on the bimetal Q [J] is given by

$$Q = C \cdot \delta T \tag{3}$$

with C [J K^{-1}] the heat capacity for the considered temperature rise δT [K].

Through the use of the *Joule-Lenz's law* it is possible to derive the heat Q^+ [J] transferred to the bimetal, with electrical resistance R [Ω], by the flowing current I [A] in the time period δt [s]

$$Q^+ = RI^2 \cdot \delta t. \tag{4}$$

Finally, the heat loss Q^- [J] due to thermal conduction is given by the *Fourier's Law* where the bimetal component was approximated as a homogeneous material of 1-D geometry with surface S [m^2], thermal conductance h [W m^{-2} K^{-1}], and temperature difference between the bimetal and the other components δT_2 [K]:

$$Q^- = hS \cdot \delta t \cdot \delta_2 T. \tag{5}$$

This loss term was considered due to the presence of external elements in contact with the bimetal (other components of the thermal unit such as junction surfaces and rivets). On the other hand, convection and radiation heat losses were not considered relevant. Thus, the balance of energy equation becomes:

$$C \cdot \delta T = RI^2 \cdot \delta t - hS \cdot \delta t \cdot \delta T_2. \tag{6}$$

Considering a linear dependence of the electrical resistance with respect to the temperature

$$R = aT + b, \tag{7}$$

it is possible to derive the discrete-time dynamical equation of the electro-thermal model as

$$T_k = \alpha \cdot U_{k-1} T_{k-1} + \beta \cdot U_{k-1} + (1-\gamma) \cdot T_{k-1} + \gamma \cdot T_{k-2} \tag{8}$$

where k is the discrete-time index, $U_k = I_k^2$, $\delta T_2 = T_{k-1} - T_{k-2}$, and $\delta t = t_s$. The coefficients $\alpha = at_s/C$, $\beta = bt_s/C$, and $\gamma = hSt_s/C$ encode physical and geometrical parameters of the bimetal.

These parameters present an high variability due to the manufacturing process of the bimetallic strip and the assembly process of the circuit breaker thermal component. Thus, characterizing the bimetal variability by means of a simulation model is useful to study the bimetal population.

3.2 Thermo-mechanical model

Consider a bimetallic strip composed by two metallic layers, and let α_2 [K^{-1}], m_2 [m], n_2 [N m^{-2}] be the thermal expansion coefficient, thickness and Young's modulus of the *active component*. Likely, let α_1 [K^{-1}], m_1 [m], n_1 [N m^{-2}] be the thermal expansion coefficient, thickness and Young's modulus of the *passive component*. A general equation for the curvature of a *uniformly heated, two-layers* bimetallic strip can be defined by relying on the theory of elastic beams, see Timoshenko (1925):

$$\frac{1}{\rho} = \frac{6 \cdot (\alpha_2 - \alpha_1) \cdot \Delta T \cdot (1+m)^2}{h\left[3(1+m)^2 + (1+mn)\cdot\left(m^2 + \frac{1}{mn}\right)\right]}, \tag{9}$$

where ρ is the curvature ray, $m = \frac{m_1}{m_2}$ and $n = \frac{n_1}{n_2}$. Considering the boundary condition at fixed support and letting the other end of the beam free to bend (*cantilever model*, see Webster (1999); Goodno and Gere (2018)), it is possible to derive an approximation between the strip curvature ρ and the relative deflection Δx as

$$\Delta x \simeq \frac{L^2}{2\rho}. \tag{10}$$

The *static* equation governing the bimetal displacement and temperature at the end of the trip is obtained as

$$\Delta x = \frac{3L^2 \cdot (\alpha_2 - \alpha_1) \cdot (1+m)^2}{h\left[3(1+m)^2 + (1+mn)\cdot\left(m^2 + \frac{1}{mn}\right)\right]} \cdot \Delta T \tag{11a}$$

$$\approx \lambda \cdot \Delta T,$$

where the approximation follows from the consideration that, with respect to the application range of temperature, all the parameters in (11) can be considered as constants.

Fig. 6 displays the values of Δx and ΔT for all the curves in the dataset, where we estimated $\hat{\lambda}$ via least-squares. The resulting line through the origin does not represent the experimental data well. In order to better model the thermo-mechanical relation, a *black-box* first order dynamical model is proposed

$$x_k = \delta \cdot T_{k-1} + \zeta \cdot x_{k-1}, \tag{12}$$

where x_k is the deflection value at time k and $\delta, \zeta \in \mathbb{R}$ are unknown parameters to be estimated from data.

The ARX structure of the model in (12) was chosen as the simplest structure to cope both with the temperature-deflection relation expected from the bimetallic effect (Khadkikar (1993); Webster (1999)) as well as to add a dynamic fade-memory contribution. Model order selection was guided by the parsimony principle given the limited amount of data available, leading to a first order model. Nonetheless, a second-order model was also tried but with unsatisfactory results compared to the higher complexity.

In some tests the deflection curve presents an undesired behaviour, visible in Fig. 7, where the deflection curve changes its steep angle when the disturbance occurs. An explanation of this phenomenon can be found in the resistance on contact acting between the bending bimetal and the revolving shaft of the trip unit. It is therefore important, in order to model it appropriately, to detect the

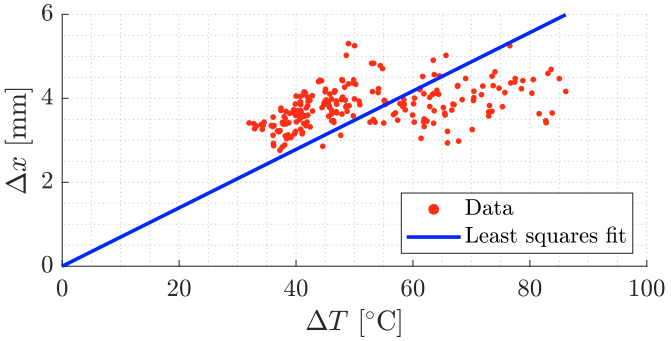

Fig. 6. Evaluation of (11) for experimental values of ΔT and Δx.

occurrence and magnitude of this event. To this end, an algorithm based on the derivative of the deflection signal x is proposed, where the detection of the start and stop times t_1^* and t_2^* of the disturbance is carried out by means of a threshold, heuristically tuned on the experimental data.

Remark 3. (*Mechanical disturbance*) The disturbance phenomenon is not always present, and it probably depends on the interactions between the 3 bimetallic strips (one for each phase of the circuit breaker). We leave the investigation of this topic to future research.

The final relationship between temperature rise and deflection of the bimetallic strip becomes:

$$x_k = \begin{cases} \delta \cdot T_{k-1} + \zeta \cdot x_{k-1} + \mu & \text{if disturbance is present,} \\ \delta \cdot T_{k-1} + \zeta \cdot x_{k-1} & \text{otherwise.} \end{cases}$$

where the added term μ models the external disturbance on the deflection curves.

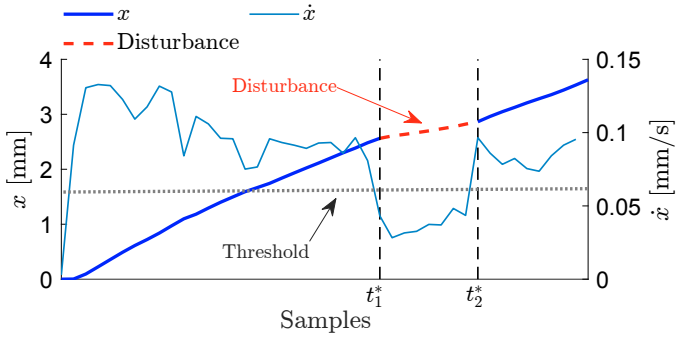

Fig. 7. Exemplification, for a single deflection curve, of the undesired disturbance and the mode of operation of detection algorithm.

4. PARAMETERS ESTIMATION

The parameters vector $\hat{\boldsymbol{\theta}}_{\text{ET}} = (\hat{\alpha}, \hat{\beta}, \hat{\gamma})$ of the electro-thermal model and the parameters vector $\hat{\boldsymbol{\theta}}_{\text{TM}} = (\hat{\delta}, \hat{\zeta}, \hat{\mu})$ of the thermo-mechanical model are *estimated separately*, for each couple of circuit breaker-phase. Let

$$\boldsymbol{\theta} = \begin{cases} \boldsymbol{\theta}_{\text{ET}} & \text{for the electro-thermal (ET) model,} \\ \boldsymbol{\theta}_{\text{TM}} & \text{for the thermo-mechanical (TM) model,} \end{cases}$$

with $\hat{\boldsymbol{\theta}}$ an estimate of $\boldsymbol{\theta}$. Thus, $\boldsymbol{\theta}$ is estimated as

$$\hat{\boldsymbol{\theta}} = \arg\min_{\boldsymbol{\theta}} V_{i,j}(\boldsymbol{\theta}), \qquad \forall (i,j) \in \mathcal{I} \times \mathcal{J} \tag{13}$$

where $\mathcal{I} = \{1, \dots, N_B\}$, $\mathcal{J} = \{1, \dots N_P\}$ and the subscript (i, j) represents the couple of the i-th circuit-breaker and j-th phase that is being considered. For the sake of notation compactness, the subscript (i, j) is detached from the parameter vector $\boldsymbol{\theta}$, i.e. $\boldsymbol{\theta}_{i,j} \equiv \boldsymbol{\theta}$.

The objective functions to be minimized are defined as:

$$V_{i,j}(\boldsymbol{\theta}) = \frac{1}{m} \sum_{h=1}^{m} \sum_{k=1}^{N_{i,j}^h} \left(e_{i,j}^h(k; \boldsymbol{\theta})\right)^2, \ \forall (i,j) \in \mathcal{I} \times \mathcal{J} \quad (14)$$

where $N_{i,j}^h$ is the number of data points of the h-th curve for the j-th phase of the i-th breaker. Since we have $N_T = 3$ curves for each breaker/phase, we employ $m = 2$ of them for *identification* and the remaining one for *validation* purposes. So, a total of $m \cdot N_B = 180$ temperature and displacement curves are employed, i.e. $m = 2$ curves for each breaker/phase couple (i, j).

The error $e_{i,j}^h(k)$ is defined as the difference between experimental data and simulated data for the considered model:

$$e_{i,j}^h(k; \boldsymbol{\theta}) = \begin{cases} T_{i,j}^h(k) - \hat{T}_{i,j}^h(k; \boldsymbol{\theta}_{\text{ET}}) & \text{for the ET model} \\ x_{i,j}^h(k) - \hat{x}_{i,j}^h(k; \boldsymbol{\theta}_{\text{TM}}) & \text{for the TM model,} \end{cases}$$

where

- $T_{i,j}^h(k)$ and $x_{i,j}^h(k)$ are, respectively, the measured temperature and displacement for the h-th curve of the j-th phase of i-th breaker;
- $\hat{T}_{i,j}^h(k; \hat{\boldsymbol{\theta}}_{\text{ET}})$ is the temperature estimated by the ET model (8), using the *simulated* step (squared current) input $U = I^2$;
- $\hat{x}_{i,j}^h(k; \hat{\boldsymbol{\theta}}_{\text{TM}})$ is the deflection estimated by the TM model (12), using the *measured* temperature input $T_{i,j}^h(k)$.

Remark 4. Since U_k is not known apart from its amplitude, this input signal is simulated equally for each breaker i and phase j.

Remark 5. Even if each circuit breaker has $N_P = 3$ phases (i.e. N_P bimetallic strips that bend together), we here consider the single phases in separately from their breaker. We left improvements and extensions to future researches.

Summarizing, we estimated $N_B \cdot N_P = 90$ couples of $\left(\hat{\boldsymbol{\theta}}_{\text{ET}}, \hat{\boldsymbol{\theta}}_{\text{TM}}\right)$ parameters, one for each couple of circuit breaker/phase. The estimation procedure was carried out by the MATLAB optimization function `fmincon`.

5. RESULTS

Identification results on *estimation data* for the electro-thermal and thermo-mechanical models are reported in Fig. 8 and Fig. 9, respectively, for a single phase of a single breaker. Two datasets are shown since m tests are performed for each breaker-phase configuration.

We employed the *validation data* to separately assess:

- the electro-thermal (ET) model
- the thermo-mechanical (TM) model
- the *overall* electro-mechanical (EM) model, that estimates the deflection $\hat{x}$ given the (simulated step input $U = I^2$, see Fig. 10.

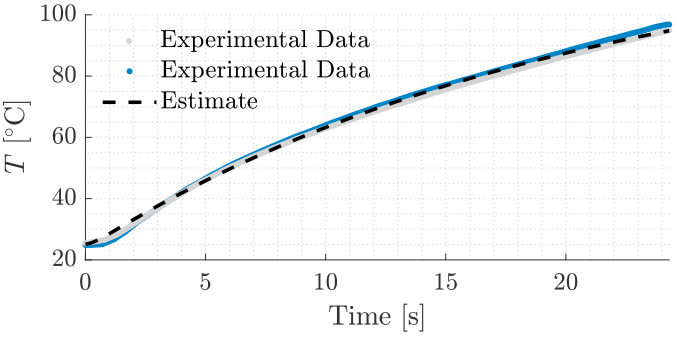

Fig. 8. Example of an estimated temperature curve for a single phase of a single circuit breaker.

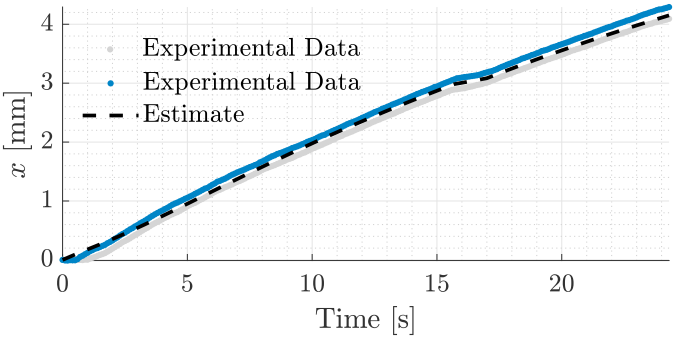

Fig. 9. Example of an estimated deflection curve for a single phase of a single circuit breaker.

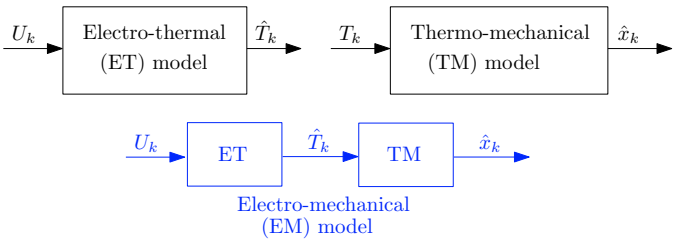

Fig. 10. Block diagrams of the Electro-Thermal, Thermo-Mechanical, and overall Electro-Mechanical models.

To this end, the following Root Mean Square Error (RMSE) costs are computed for each of the 90 couples of circuit breaker/phase:

$$J_{i,j}^{\text{ET}}\left(\hat{\boldsymbol{\theta}}_{\text{ET}}\right) = \sqrt{\frac{1}{N_{i,j}^*} \sum_{k=1}^{N_{i,j}^*} \left[T_{i,j}^*(k) - \hat{T}_{i,j}^*(k; \hat{\boldsymbol{\theta}}_{\text{ET}})\right]^2} \quad (15a)$$

$$J_{i,j}^{\text{TM}}\left(\hat{\boldsymbol{\theta}}_{\text{TM}}\right) = \sqrt{\frac{1}{N_{i,j}^*} \sum_{k=1}^{N_{i,j}^*} \left[x_{i,j}^*(k) - \hat{x}_{i,j}^*(k; \hat{\boldsymbol{\theta}}_{\text{TM}})\right]^2} \quad (15b)$$

$$J_{i,j}^{\text{EM}}\left(\hat{\boldsymbol{\theta}}_{\text{EM}}\right) = \sqrt{\frac{1}{N_{i,j}^*} \sum_{k=1}^{N_{i,j}^*} \left[x_{i,j}^*(k) - \hat{x}_{i,j}^*(k; \hat{\boldsymbol{\theta}}_{\text{EM}})\right]^2} \quad (15c)$$

where $\hat{\boldsymbol{\theta}}_{\text{EM}} = \left[\hat{\boldsymbol{\theta}}_{\text{ET}} \quad \hat{\boldsymbol{\theta}}_{\text{TM}}\right]$, and

- $T^*_{i,j}(k)$ and $x^*_{i,j}(k)$ are, respectively, the measured temperature and displacement for the h-th curve of the j-th phase of i-th breaker on *validation data*;
- $\hat{T}^*_{i,j}(k, \hat{\boldsymbol{\theta}}_{\mathrm{ET}}) = \hat{T}^h_{i,j}(k, \hat{\boldsymbol{\theta}}_{\mathrm{ET}})$ is the temperature estimated by the ET model (8), using the *simulated* step (squared current) input $U = I^2$;
- $\hat{x}^*_{i,j}(k, \hat{\boldsymbol{\theta}}_{\mathrm{TM}})$ is the deflection estimated by the TM model (12), using the *measured* validation temperature input $T^*_{i,j}(k)$.
- $\hat{x}^*_{i,j}(k, \hat{\boldsymbol{\theta}}_{\mathrm{EM}})$ is the deflection estimated by the overall EM model, using the *estimated* validation temperature input $\hat{T}^*_{i,j}(k, \hat{\boldsymbol{\theta}}_{\mathrm{ET}})$.

The boxplots of the validation errors are reported in Fig. 11, where it is possible to notice that:

- the RMSE of the TM model is very similar to the error of the EM model, meaning that the ET model attains very good results;
- the ET model has a median RMSE of 0.7 °C, while the TM and EM models have a median RMSE of 0.08 mm, all with very few outliers.

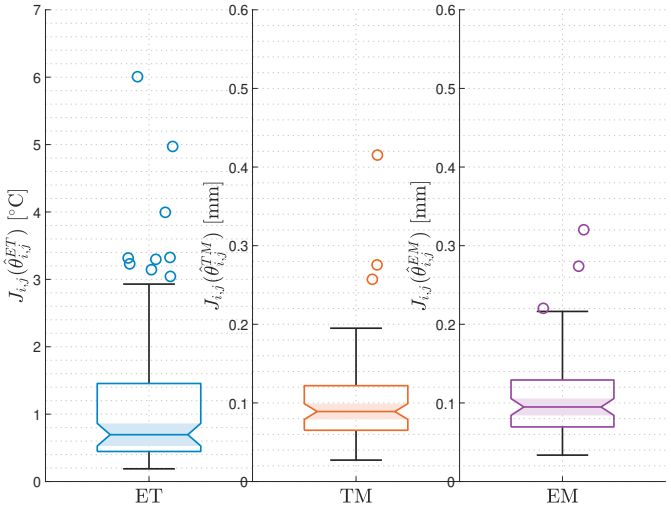

Fig. 11. From left to right, the RMSE of the Electro-Thermal, Thermo-Mechanical, and overall Electro-Mechanical models computed on the validation dataset.

6. CONCLUSIONS

This paper presented a dynamical model for the dynamics of the bimetallic strip in industrial circuit breakers. The proposed model consists in two submodels; the first explains the electro-thermal relationship relying on the physical relations of the heat dynamics. The second describes the thermo-mechanical relationship directly from the experimental data by means of a black-box model. Even if the derivation process introduces some assumptions and approximations, the overall electro-thermo-mechanical model proved to perform well on the limited validation dataset available.

Future research is devoted to: (i) study the relation between the three bimetallic strip inside each circuit breaker; (ii) develop an automatic calibration of the devices and their experimental validation.

REFERENCES

Balestrero, A., Ghezzi, L., Popov, M., and van der Sluis, L. (2010). Current interruption in low-voltage circuit breakers. *IEEE Transactions on Power Delivery*, 25(1), 206–211. doi:10.1109/TPWRD.2009.2035298.

Čepon, G., Starc, B., Zupančič, B., and Boltežar, M. (2017). Coupled thermo-structural analysis of a bimetallic strip using the absolute nodal coordinate formulation. *Multibody System Dynamics*, 41(4), 391–402.

Goodno, B.J. and Gere, J.M. (2018). *Mechanics of materials*. Cengage Learning, Boston, MA.

Khadkikar, P. (1993). The principles and properties of thermostat metals. *Journal of Metals*, 45(6), 39–42. doi: 10.1007/BF03223309.

Pionke, C.D. and Wempner, G. (1991). The various approximations of the bimetallic thermostatic strip. *Journal of Applied Mechanics*, 58(4), 1015–1020. doi: 10.1115/1.2897676.

Ross, D.S., Cabal, A., Trauernicht, D., and Lebens, J. (2005). Temperature-dependent vibrations of bilayer microbeams. *Sensors and Actuators A: Physical*, 119(2), 537–543.

Sedighi, M. and Dardashti, B.N. (2012). A review of thermal and mechanical analysis in single and bi-layer plate. *Materials Physics and Mechanics*, 14(1), 37–46.

Suocheng, W., Yongping, H., and Shuangjie, L. (2015). The design and analysis of a mems electrothermal actuator. *Journal of Semiconductors*, 36(4), 044012.

Timoshenko, S. (1925). Analysis of bi-metal thermostats. *Journal of the Optical Society of America*, 11(3), 233–255. doi:10.1364/josa.11.000233.

Webster, J. (1999). *The measurement, instrumentation, and sensors handbook*. CRC Press published in cooperation with IEEE Press, Boca Raton, Fla.

Zou, Q., Sridhar, U., and Lin, R. (1999). A study on micromachined bimetallic actuation. *Sensors and Actuators A: Physical*, 78(2), 212 – 219. doi:10.1016/S0924-4247(99)00236-8.